Sensors & Actuators: A. Physical 378 (2024) 115826

Contents lists available at ScienceDirect

Sensors and Actuators: A. Physical

journal homepage: www.journals.elsevier.com/sensors-and-actuators-a-physical

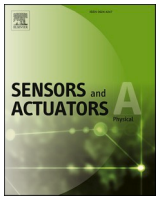

High performance PVC/ $[AMI]_mNTF_2$ ionic gel sensors for smart wearable applications

Yi Li [a,b,c,*], Ziqian Zhang [a,b], Lixiang Zhu [a,b], Hangzhong Zhu [a,b], Xia Zhang [d,**], Mingfei Guo [a,b], Yanbiao Li [a,b,*], Minoru Hashimoto [e,**]

[a] Key Laboratory of Special Purpose Equipment and Advanced Processing Technology of the Ministry of Education, Zhejiang University of Technology, Hangzhou 310023, China
[b] Zhejiang Provincial Key Laboratory of Special Purpose Equipment and Advanced Processing Technology, Zhejiang University of Technology, Hangzhou 310023, China
[c] Ninghai ZJUT Academy of Science and Technology, Ningbo 315615, China
[d] School of Mechatronics and Vehicle Engineering, Chongqing Jiaotong University, Chongqing 400074, China
[e] Faculty of Textile Science and Technology, Shinshu University, 3-15-1 Tokida, Ueda, Nagano 386-8567, Japan

ARTICLE INFO

Keywords:
PVC ionic gel
Strain sensor
Mechanical stretching
Flexible electronic devices
Motion monitoring

ABSTRACT

Plasticized polyvinyl chloride (PVC) gel as an electroactive polymer material has attracted increasing interest for the construction of flexible devices with the integration of actuation and self-sensing. However, the insufficient sensing ability of traditional PVC gels limits their applications. In this paper, a PVC ionic gel sensor based on the physical blending of PVC gel and the ionic liquid 1-allyl-3-methylimidazolium bisimide ($[AMI]_mNTF_2$) is presented. With the addition of ionic liquids, the PVC molecular chains and ions formed stable conductive pathways, resulting in increased conductivity and sensing performance of the PVC gel. The proposed sensor exhibits excellent sensing properties of high resolution (0.12 %) and fast response time (95 ms), along with high sensitivity (GF=27.8), which is more than seven times that of the traditional PVC gel. Furthermore, it was successfully utilized for human motion detection and remote control of a robotic hand, demonstrating the feasibility of the sensor for smart wearable applications in the future.

1. Introduction

During the last decades, electroactive materials, which are regarded as the ideal choice for smart materials, have demonstrated numerous advantageous properties, including excellent actuation capabilities and biocompatibility, leading to their widespread application in assisted rehabilitation[1], haptic perception[2,3] and soft robotics[4,5]. Despite their potential, most of these materials lack sensing characteristics [6–10], hindering their ability to fulfill the demands of real-field applications, resulting in many attempts to enhance their sensing properties[11]. For example, addition of nanoparticles to ionic polymer metal composites (IPMC) to enhance their electrical activity[12], incorporation of conductive fillers into dielectric elastomers to improve conductivity[13], and introduction of new elements by alloying in shape memory alloys (SMA) to improve their sensing properties[14]. These efforts have succeeded in improving the sensing range and sensitivity of the electroactive materials. Nevertheless, the sensing properties of most electroactive materials are either limited by their slow response[15,16] or weak sensing signals[17], which restricts their practical applications.

Recently, PVC gels have attracted considerable interest in the field of electroactive materials due to their distinctive actuation properties[18], which make them competitive for various applications, including soft robots[19], smart wearable gears[20], artificial muscles[21] and other cutting-edge fields[22]. Moreover, various studies have been conducted to improve the PVC gel sensing characteristics through their piezoresistive and strain-resistive properties[23]. Hwang et al.[24] utilized the piezoresistive property of PVC gel when voltage was applied, and the gel could quickly detect collisions, show 4.78 times a sensitivity. But one major limitation of this method is its inability to offer constant detection, which makes it difficult to use. In response, researchers have focused on the ability of PVC gels to change their internal impedance through deformation, while adding conductive factors to enhance their

* Corresponding authors at: Key Laboratory of Special Purpose Equipment and Advanced Processing Technology of the Ministry of Education, Zhejiang University of Technology, Hangzhou 310023, China
** Corresponding authors.
E-mail addresses: ly17@zjut.edu.cn (Y. Li), zhangx82@cqjtu.edu.cn (X. Zhang), lybrory@zjut.edu.cn (Y. Li), hashi@shinshu-u.ac.jp (M. Hashimoto).

https://doi.org/10.1016/j.sna.2024.115826
Received 27 June 2024; Received in revised form 8 August 2024; Accepted 19 August 2024
Available online 22 August 2024

sensing capabilities. He et al.[25] used the ionic liquid 1-ethyl-3-methylimidazole thiocyanate as a dielectric medium to realize an excellent ionic gel with a high linearity, high response and stable sensing performance. Song et al.[26] have formulated an ionic gel by incorporating 1-ethyl-3-methylimidazolium bisimide, which retains its elasticity after numerous cycles of stretching and possesses high transparency. While the resolution of PVC ionic gel is not great and their sensitivity is low (gauge factor GF<5)[25,26], it remains a challenge to achieve high resolution, high reproducibility, and high sensitivity in PVC ionic gels [27].

We developed a novel PVC ionic gel based on the addition of ionic liquid modification to solve the problem of poor sensing properties. We chose alkenyl ionic liquids with high solubility and conductivity and three different molecular weights: $[AMI]_mCl$, $[AMI]_mBF_4$, and $[AMI]_mNTF_2$. Moreover, based on the differences in chemical structures, we compared one-substituted($[MI]_mCl$) and two-substituted($[BMI]_mCl$) imidazolium-based ionic liquids. The final comparison revealed that $[AMI]_mNTF_2$ was more suitable for PVC gels. Using the physical blending method, the ionic liquid 1-allyl-3-methylimidazolium bisimide ($[AMI]_mNTF_2$) was introduced into the PVC/DBA gels. As a plasticizer, DBA can change the physical properties of PVC through hydrogen bonding and van der Waals force interactions, effectively improving the mechanical characteristics of the material. The ionic liquid has a better electrical conductivity and solubility, and can be dissolved in the PVC solution to form a uniform ionic gel. The internal PVC molecular network and the ions formed a conductive path and improved the conductivity of the gels. Importantly, the electrical and mechanical properties of PVC ionic gels can be modified by adjusting the ionic liquid type, plasticizer content and crosslinking network density. Finally, it exhibits high sensitivity (GF=27.8), 5–6 times higher performance than the same type of ionic gel, and more than 7 times higher than traditional PVC gel, along with high resolution (0.12 %) and fast response time (loading: 95 ms, unloading: 98 ms). Furthermore, PVC ionic gel sensors have been utilized in wearable devices to detect human joint motion. The successful verification of signal detection, including finger bending, writing, speaking, leg movements, and remote control of robotic hand, clearly demonstrates that PVC ionic gels have great potential to overcome certain limitations in real applications.

2. Experimental section

2.1. Materials

PVC powder (polyvinyl chloride) (PVC), CAS 9002–86–2), plasticizer (dibutyl adipate (DBA), CAS 105997, 96 %), and solution (tetrahydrofuran (THF), CAS 109999, 99.9 %) were purchased from Sigma-Aldrich. A flexible electrode material (Oil compound KS- 660) was purchased from Shibosh-i Chemical. N-Methylimidazolium chloride($[MI]_mCl$), 1-Allyl-3-methylimidazolium chloride ($[AMI]_mCl$), 1-butyl-3-methylimidazolium chloride($[BMI]_mCl$), Allyl-3-methylimidazolium tetrafluoroborate ($[AMI]_mBF_4$), 1-Allyl-3-methylimidazolium bis((trifluoromethyl)sulfonyl)imide ($[AMI]_mNTF_2$) were purchased from Qingdao Oli New Material Co. Ltd. ionic liquid, and all chemicals were not further purified.

2.2. Fabrication of PVC Ionic gel membrane

PVC ionic gel solutions were prepared following a previously reported method[28], with some modifications(Fig. S1). First, the PVC powder was dissolved in THF and centrifuged. The resulting solution was stirred at 3000 rpm for 6 minutes. The DBA solution was then mixed with the PVC/THF solution and the mixture was centrifuged for 6 minutes. Next, a proportional amount of good ionic liquid was added, and the resulting PVC/DBA/THF/ILs solution was stirred at 1500 rpm for 48 hours at room temperature. The PVC gel was molded using a solution casting process. The gel mixture was poured into a stainless steel evaporating dish, and the shape of the dish helped to solidify and shape the solution. THF was completely volatilized in a constant-temperature incubator at 24°C. After 48 hours, the PVC gel was molded. The experimental preparation method is illustrated in Fig. S1. The ionic liquid content and amount of plasticizer DBA are related to the molecular gap of plasticized PVC[29], which has a significant impact on the mechanical and electromechanical properties of PVC gels[30].

The weight ratio of PVC, DBA, and IL in PVC/DBA/IL gels was set to 1:4:x in this study. PVC/DBA gel samples with varying IL contents were named as P/IL wt% gels. For instance, PVC/DBA gel samples containing 0.8 wt% $[AMI]_mNTF_2$ were named as P/ $[AMI]_mNTF_2$ 0.8 wt%. The weight ratios for other ionic liquid types were also 0.8 wt%, and they were named as P/IL name weight% gels, such as P/$[AMI]_mBF_4$ 0.8 wt%. PVC and DBA were combined without the use of an ionic liquid in a weight ratio of 1:x for PVC and DBA, where x represents the weight of DBA relative to PVC. For example, a ratio of 1:4 for PVC to DBA was named PVC14.

2.3. Morphological characteristics of PVC ionic gels

Utilizing a Thermo Scientific Nicolet iS20, the analysis was performed with a resolution of 4 cm^{-1} over 32 scans spanning a wavenumber range of 400–4000 cm^{-1}. This technique is instrumental in characterizing and analyzing the chemical structures of PVC, DBA, PVC gels, ionic liquids, and PVC ionic gels. Complementary to FTIR, X-ray diffraction (XRD) tests were performed using a Rigaku Ultima IV diffractometer. By examining the 2θ angle range of 10–60°, we probed the crystallization processes within the PVC ionic gels, particularly focusing on the variations induced by different ionic liquid mass ratios. Furthermore, the optical properties were assessed using UV–visible (UV-Vis) absorption spectra acquired with a Shimadzu UV-3600i Plus instrument in T mode within a testing range of 300–800 nm. To investigate the impact of ionic liquid incorporation on the PVC gel interface, samples with varying IL concentrations of ionic liquids were examined. The surface morphology was examined and characterized using a scanning electron microscope (ZEISS Sigma 300) at various magnifications.

2.4. Mechanical tests

To evaluate the mechanical properties of the PVC ionic gels, we performed uniaxial tensile tests on PVC gel membranes with different dibenzylamine (DBA) ratios and PVC ionic gel membranes with different types of ionic liquids. Tests were performed using an electronic universal testing machine (CMT6103 MTS). The force-measuring element of the system had a capacity of 10 N and an accuracy of 0.01 mN, and the displacement-measuring element, with a capacity of 10–800 mm and an accuracy of 0.032 μm, allowed for the simultaneous measurement of force and deformation of the specimens. The PVC gel film samples were fashioned into 3-type dumbbell shapes, each with a total length of 50 mm and thickness of 500 μm, as shown in Fig. S2. Uniaxial stretching of PVC gel films was performed at a rate of 10 mm/min at room temperature. In particular, the rheological properties of the PVC gels were studied using a rheometer (HAAKE MARS 60), which made it possible to study the changes in the internal loss and storage moduli under loading.

2.5. Electrical measurements

An electrochemical station tester was used to characterize the conductivity of the PVC ionic gels with different ionic liquids and ionic liquid contents. Conductivity (σ, S/cm) was calculated using the following formula:

$$\sigma = L/(R \times A) \quad (1)$$

Where, L is the fixed length between the two probes and R (Ω) and A (cm^2) are the resistance and cross-sectional area of the gel sample,

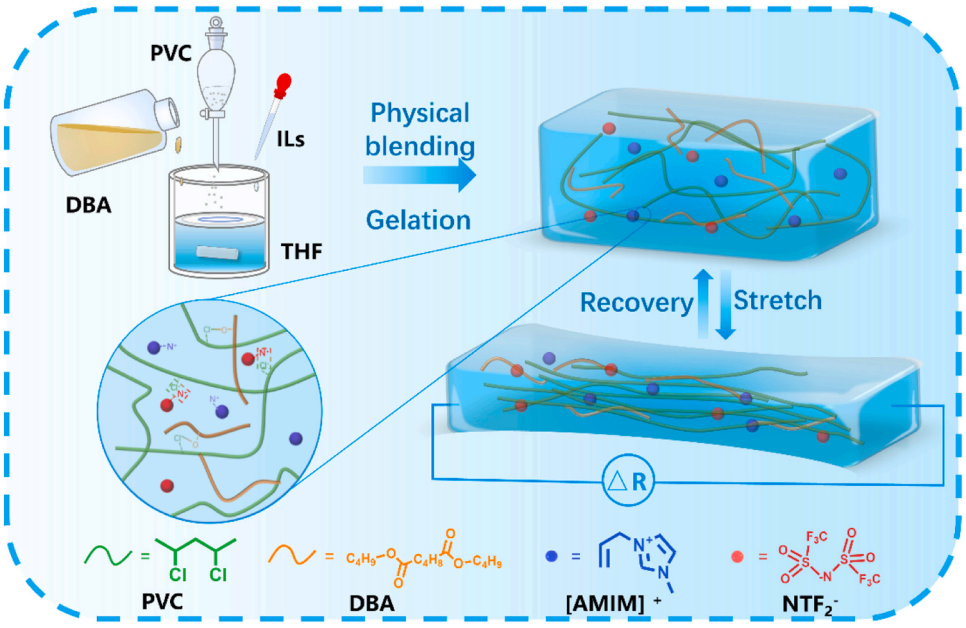

Fig. 1. Sensing mechanism diagram.

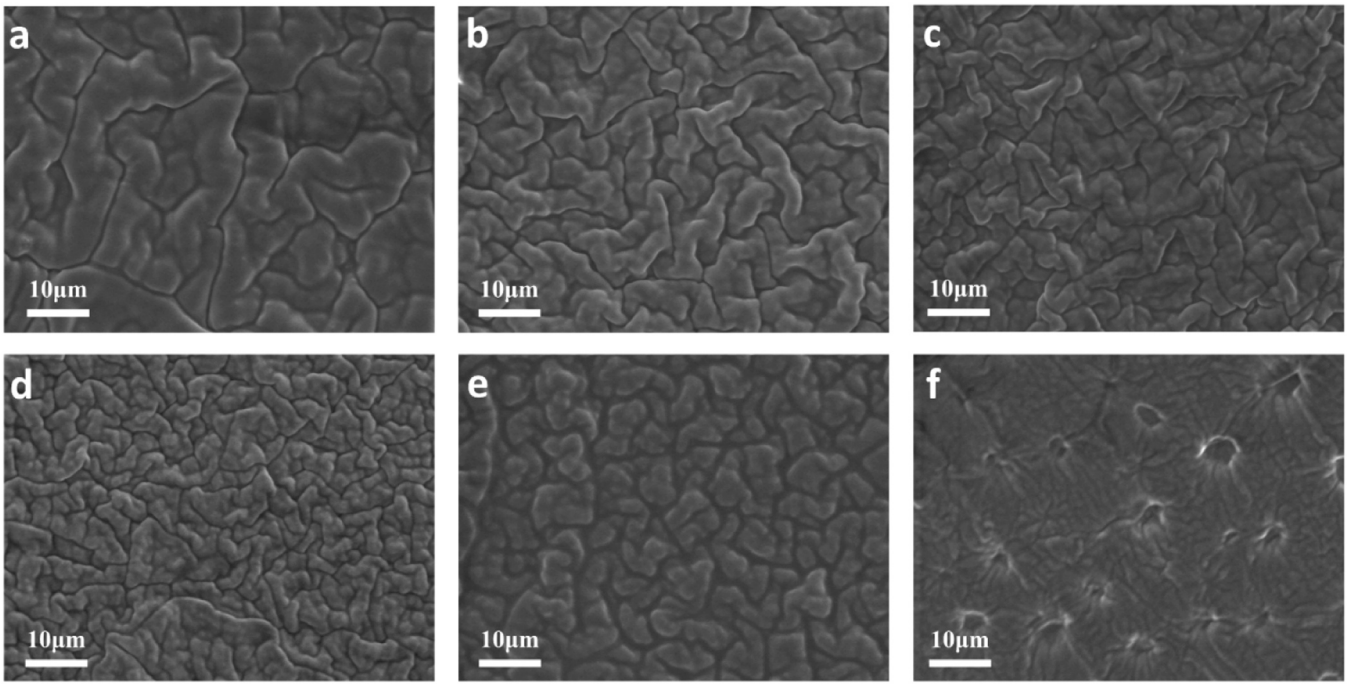

Fig. 2. Microstructure of the PVC ionic gel.(a) PVC14 gel. (b) P/ $[AMI]_mNTF_2$ ionic gel 0.2 wt%. (c) P/ $[AMI]_mNTF_2$ ionic gel 0.4 wt%. (d) P/ $[AMI]_mNTF_2$ ionic gel 0.8 wt%. (d) P/ $[AMI]_mNTF_2$ ionic gel 2 wt%. (d) P/ $[AMI]_mNTF_2$ ionic gel 4 wt%.

respectively. Impedance tests were performed using an impedance analyzer (E4990A) to obtain the electrochemical data of the PVC ionic gel, which led to an equivalent circuit model of the PVC ionic gel.

To test the change in resistance of the gel during the strain process, an independently designed experimental test platform was used, as shown in Fig. S4. Specific strains were applied to the ionic gel and the resistance change signals of the gel were recorded using an LCR tester (BK) instrument. The PVC ionic gel was attached to the human body as a wearable sensor and was connected to the tester through wires to detect body movements. The output signal was recorded as the change in resistance using the following equation:

$$GF = (\Delta R/R_0)/\varepsilon \quad (2)$$

Where, GF is the sensitivity of the PVC ionic gel; R and R_0 are the resistances after and before applying strain on the PVC ionic gel, respectively; and ε is the strain applied to the gel.

3. Results and discussion

3.1. Material characterization of PVC ionic gels

This study aimed to investigate the effects of DBA content and ionic

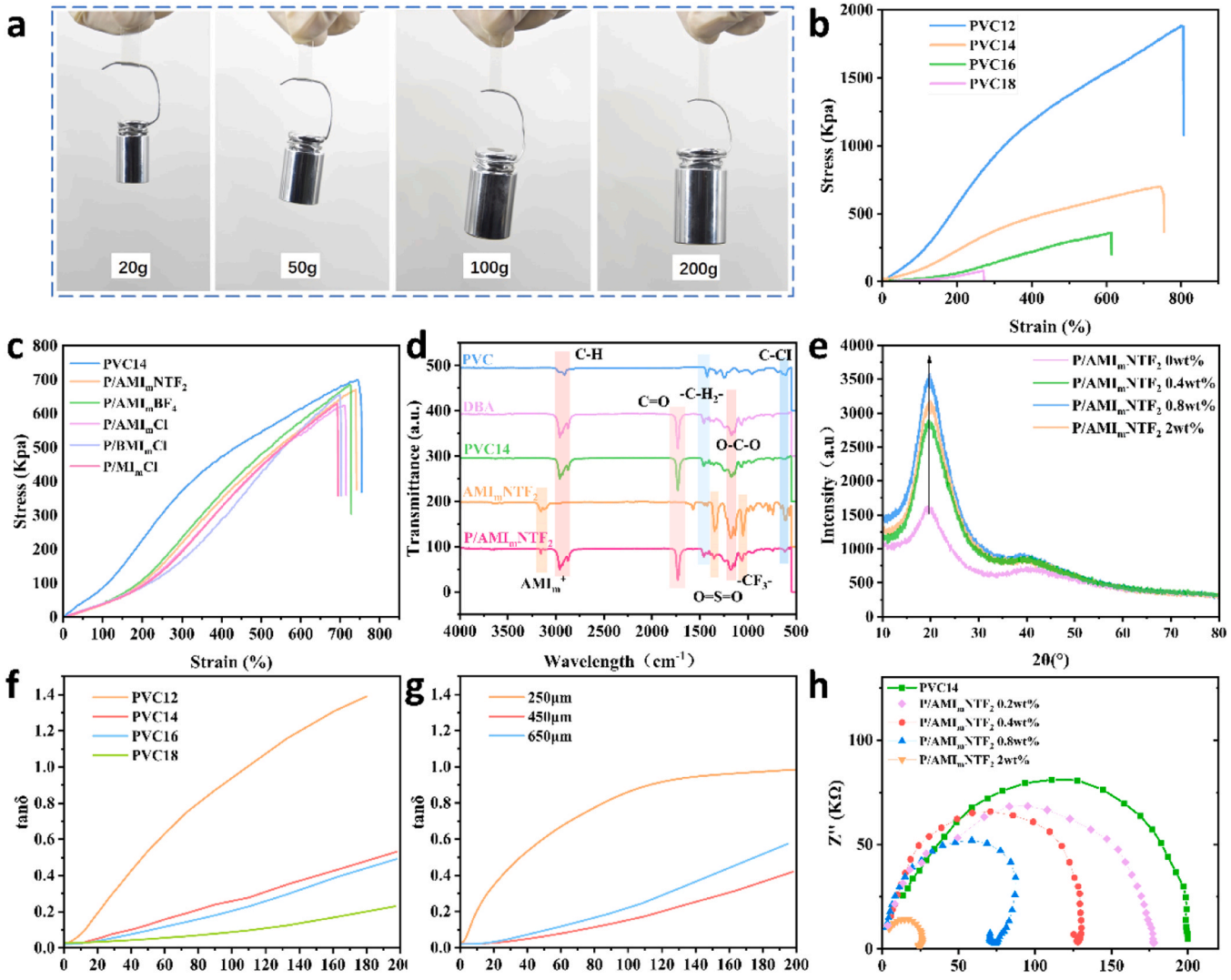

Fig. 3. Material characterization of PVC ionic gels. (a) Diagrams of the gel in suspension of 20 g, 50 g, 100 g, and 200 g weights. (b) Stress-strain curves of PVC gels with different DBA contents. (c) Stress-strain curves of PVC gels with different ionic liquid additions. (d) Fourier infrared spectral analysis of PVC, DBA, PVC gel, IL and PVC ionic gel. (e) X-ray diffractograms for different ionic liquid concentrations. (f) Mechanical loss of PVC gel at 0–200 % strain for different DBA contents. (g) Mechanical losses of PVC gels with different thicknesses under 0–200 % strain. (h) Impedance analysis for different ionic liquid concentrations.

liquid type on the mechanical properties of ionic gels. The P/[AMI]$_m$NTF$_2$ ionic gel demonstrated remarkable tensile resistance and progressive elongation without fracturing under incremental load masses of 20 g, 50 g, 100 g, and 200 g, as shown in Fig. 3**a**. Mechanical testing of both PVC and ionic gels was performed using an electronic universal testing machine, and tensile assessments were performed on standard dumbbell-shaped specimens (Fig. S2), at a velocity of 160 mm/min. The resulting tensile stress-strain relationship is shown in Fig. 3**b**. The effect of DBA content on the mechanical properties of the PVC gels was investigated. It was found that the PVC 12 gels had a peak tensile elongation of 801 % and a maximum tensile stress of 1885kPa, while the PVC 14 gels had a maximum elongation of 740 % and a stress of 670 kPa.

Notably, an increase in the DBA content corresponds to a reduction in both the stress and strain peaks of the PVC gels. Fig. 3**c** shows that the incorporation of different types of ionic liquids negatively affected the mechanical robustness of the PVC ionic gels. The presence of DBA and ionic liquids within the solid matrix of the physically crosslinked polymer network was found to reduce the mechanical properties, presumably because of the space occupied within the network, which otherwise contributes to its structural integrity. Fourier-transform infrared spectroscopy (FT-IR) was employed to analyze the compositional intricacies of the ionic gels for PVC, DBA, PVC14, [AMI]$_m$NTF$_2$, and P/[AMI]$_m$NTF$_2$. As illustrated in Fig. 3**d**, the PVC14 spectrum exhibited characteristic absorption peaks. The peaks at 2958 cm^{-1} and 2873 cm^{-1} are indicative of methyl (-CH$_3$-) stretching vibrations, whereas the peak at 1730 cm^{-1} aligns with the ester (C═O) telescopic vibration. The absorption at 1460 cm^{-1} corresponds to methylene (-CH$_2$-) bending vibrations, and the peaks at 1172 cm^{-1}, 1143 cm^{-1}, and 1022 cm^{-1} were attributed to C-O telescopic vibrations. The peak at 1064 cm^{-1} represents C-C telescopic vibrations and the peak at 693 cm^{-1} is associated with C-Cl vibrations. In contrast, the P/[AMI]$_m$NTF$_2$ spectrum differs notably from that of PVC14, with the imidazole ring and C-H in ionic liquids manifesting at 3155 cm^{-1} and 3116 cm^{-1}. The peak at 1576 cm^{-1} corresponded to the backbone vibration of the imidazole ring, and the enhanced peak at 1355 cm^{-1} was primarily due to the antisymmetric telescopic vibration of O═S═O. Additionally, the peak at 1176 cm^{-1} was attributed to the antisymmetric stretching vibration of O═S═O and the stretching vibration of CF$_3$, whereas the peak at 1063 cm^{-1} was due to the stretching vibrations of C-N and S-N. This analysis substantiates the presence of the ionic liquid in the form of ions and chemical bonds within the gel, which increases the electrical conductivity of the PVC ionic gel. The incorporation of different ionic liquids, each with different ions or functional groups, is shown in Fig. S7, and were not completely retained in the PVC gels. Consequently, these

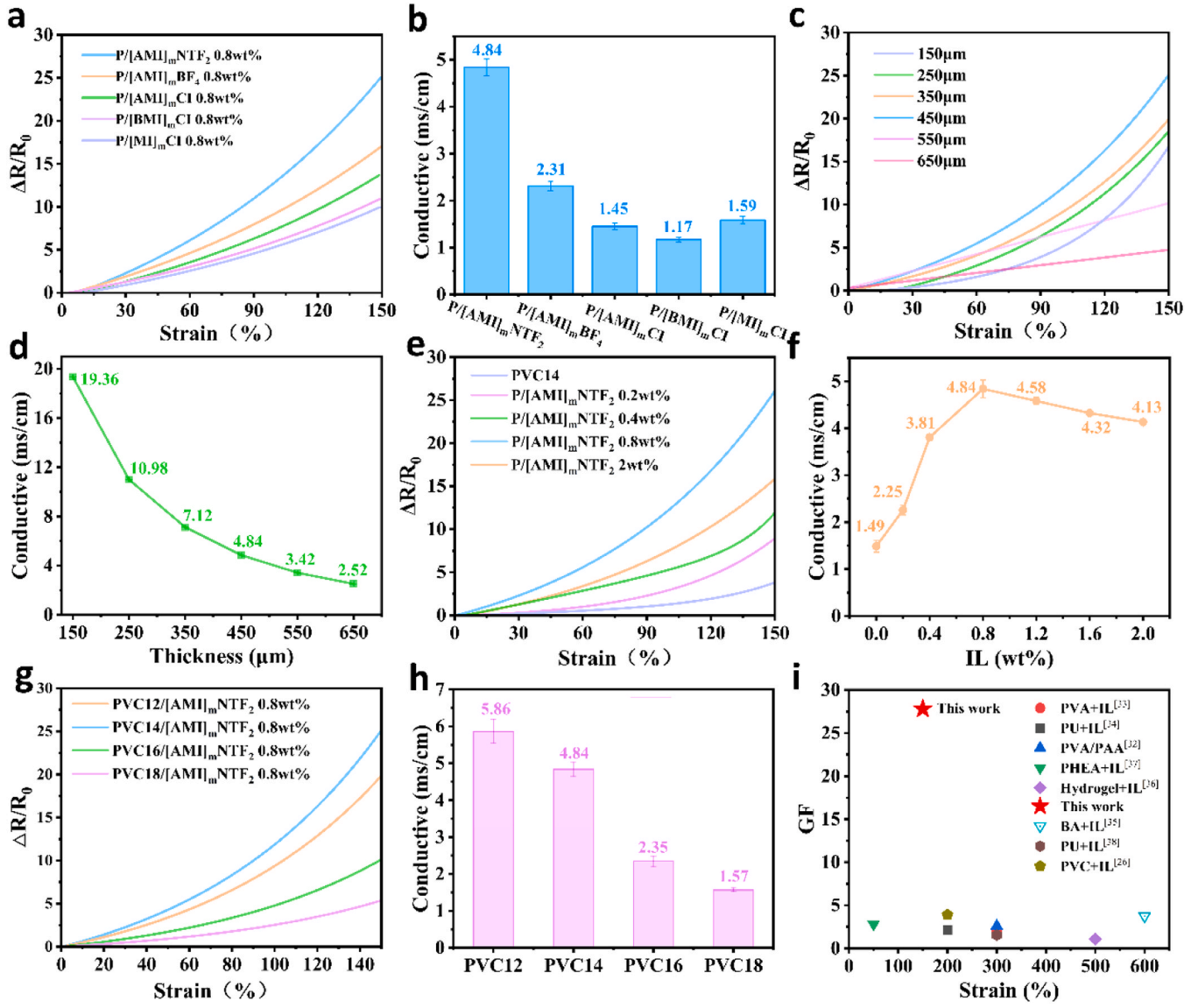

Fig. 4. Performance modulation of PVC ionic gel. (a) Sensitivity of PVC ionic gels for different ion types. (b) Conductivity of PVC ionic gels for different ion types. (c) Sensitivity of PVC ionic gels with different thicknesses. (d) Conductivity of PVC ionic gel at different thicknesses. (e) Sensitivity of PVC ionic gels at different ionic liquid concentrations. (f) Conductivity of PVC ionic gels at different ionic liquid concentrations. (g) Sensitivity of PVC ionic gels with different DBA contents. (h) Conductivity of PVC ionic gels with different DBA contents. (I) Performance comparison of PVC ionic gels with other types of ionic gel [26,33–39].

variants did not achieve the heightened electrical conductivity observed in P/[AMI]$_m$NTF$_2$.

At the same time, the crystalline architecture of the PVC ionic gels was elucidated by X-ray diffraction (XRD) analysis in the 2θ range of 10–60° (Fig. 3**e**). The primary diffraction peak of the PVC gel was observed at 2θ = 19.2°. Remarkably, this peak incrementally shifted with the addition of [AMI]$_m$NTF$_2$-0.4 wt% to 19.96°, 0.8 wt% to 20.18°, and 2 wt% to 20.26°. The intermolecular spacings of the PVC gel and PVC ionic gel were determined to be 0.462 nm and 0.432 nm, respectively. This reduction in molecular spacing with the introduction of ionic liquids suggests a decrease in the distance between the gel molecules, leading to a concomitant increase in electrical conductivity.

To understand the viscoelastic properties of PVC ionic gels and to reduce their mechanical losses, we measured the dynamic viscoelasticity of PVC gels of different thicknesses and dibenzylamine (DBA) contents using a rheometer. As depicted in Fig. 3**f** and Fig. S11, PVC12 exhibited the highest mechanical loss (tanδ = G''/G'), with a tan δ value of 1.39 at 180 % strain. Similarly, Fig. 3**g** illustrates that the gel with the thinnest profile, measuring 250 μm, displayed the greatest mechanical loss for the same PVC14 ratio, with a tanδ of 0.98 at 200 % strain. These findings indicate that mechanical loss escalates with the diminution of both the DBA content and gel thickness, which in turn amplifies the viscoelastic effect. However, this enhancement may not be conducive to sensing applications of PVC ionic gels. PVC ionic gels are prominent in the field of strain sensors because of their inherent transparency, which is esthetically advantageous. Our research revealed that the integration of imidazolium-type ionic liquids not only markedly boosted the conductivity of the gels but also preserved their high transparency.

In order to quantify the optical attributes of the PVC ionic gels, we assessed their light transmittance using an ultraviolet spectrophotometer over a wavelength range of 300–800 nm. The transmittance of all the gel variants remained above 80 %, as shown in Fig. S11. The conduction mechanism of the PVC ionic gels, as depicted in Fig. S3, was predicted for the formation of a stable conductive network by the internal PVC molecular structure and ions. When strain is applied to the gel, this internal molecular interaction disrupts the charge transfer, leading to a reduction in the separation of the conductive network and a consequent increase in the resistance of the gel.

Table 1
Performance comparison of existing PVC ionic gel strain sensors.

Additives	Conductivity	Sensitivity	Strain	Stress	Range	Response time	Cycle life	Ref.
This work	4.84 ms/cm	GF=27.8	740 %	670Kpa	0–150 %	95 ms	1500	
$[EMIM^+]$ $[TFSF^-]$	13.5μs/cm	GF=5.5	315 %	40Kpa	0–200 %		6000	26
$[EMIM^+]$ $[SCN^-]$	1.1μs/cm	GF=8.1	364 %	184Kpa	0–200 %	161 ms	35,000	25
CEC	4.0×10^{-6} ms/cm	$\triangle C/C_0$= 32	456 %	1.03Mpa	0–15 mm		1400	34
$[AMIM]^+$ NTF_2		47.5 kPa^{-1}	650 %	4.3Mpa	0–2.7Kpa			32

Thus, increasing the ionic liquid concentration, reducing the gel thickness, and increasing the PVC content are strategies to promote the development of increasingly stable conductive networks within the gel, thereby enhancing its electrical conductivity. In terms of microstructure, the PVC ionic gel was subjected to scanning electron microscopy (SEM) analysis. The SEM images in Fig. 2 and Fig. S10, reveal that the PVC14 gel, when plasticized by DBA, exhibits an opening of the molecular gaps within the polymer, resulting in a surface characterized by uniform and disordered folds at the 10 μm scale. These folds potentially acted as conduits for the DBA within the PVC polymer matrix. At lower ionic liquid concentrations, specifically P/$[AMI]_mNTF_2$ at 0.2 wt% and 0.4 wt %, the surface folds diminish in size, and the density of the surface channels increases. This trend continues with higher ion concentrations; at P/$[AMI]_mNTF_2$ 0.8 wt%, the surface folds are at their smallest, and the channel density is at its highest, correlating with the ion gel's sensitivity performance data.

Nevertheless, as the ion concentration was further increased to P/$[AMI]_mNTF_2$ 2 wt%, the channel gaps widened and the folds enlarged, leading to void formation on the gel surface, which in turn diminished the sensing capabilities of the gel. The SEM analysis confirmed the formation of a PVC ionic gel network with excellent mechanical robustness and strain-sensing attributes.

In order to decipher the equivalent circuit of the PVC ionic gels, impedance spectroscopy was performed on gels with different mass fractions of ionic liquid (0.2 wt%, 0.4 wt%, 0.8 wt% and 2 wt%). The resulting Nyquist plots, as shown in Fig. 3**h**, are characterized by semicircles, each representing a parallel circuit configuration of resistors (Rct and Rs) and capacitors(C). The low-frequency trajectory of the semicircle was delineated using resistors (Rs) and constant-phase elements (CPEs). The fitted equivalent circuit models are shown in Fig. S12 exhibited notable variations that correlated with the ion content. Especially, the diameter of the high-frequency semicircle for Rct decreases as the ionic liquid mass fraction increases, indicating a significant influence on the overall impedance of the ion gel, predominantly governed by the gel's bulk resistance. Concurrently, Rs exhibited a similar trend in magnitude, albeit to a lesser extent than Rct. In addition to the Nyquist diagram, no Warburg diffusion occurred and the Impedance Mode - Frequency was analyzed as shown in Figure S15. Under low-frequency electric field, it was found that the ions acted only as dielectrics and did not migrate. At high-frequency electric field, the capacitive properties were enhanced with the increase in the IL content. This verifies the mechanism by which the ions act as dielectric to promote charge transfer.

3.2. Characterization of electromechanical properties of PVC ionic gel

PVC ionic gels based on imidazolium-type ionic liquids exhibit excellent electrical conductivity, and the sensitivity and electrical conductivity of the gels are also important indicators for evaluating sensing performance [31,32]. We designed a series of experiments to investigate the optimal parameters for the sensing properties of the PVC ionic gels. The resistance changes in the PVC ionic gels under various strain levels were quantified using a custom-built experimental setup, as illustrated in Fig. S4, in combination with an LCR tester. The sensitivity of the sensor was calculated as $GF = (\Delta R/R_0)/\varepsilon$ [33,34], where ε is the applied strain. Among the various ionic liquid compositions tested, the gel containing 0.8 wt% P/$[AMI]_mNTF_2$ demonstrated superior sensitivity and the highest conductivity, as shown in Fig. 4**b**. Supporting the findings of the FTIR analysis (Fig. S10), it was observed that the four other imidazolium-type ionic liquids did not retain their ions or functional groups entirely within the gel matrix and had no positive effect on the conductivity of the gels.

Moreover, to explore the effect of gel cross-sectional area on the conductive path and conductivity efficiency, we standardized the gel width and investigated its thickness to determine its effect on the sensitivity and conductivity of the PVC ionic gel strain sensor (Fig. 4**d**). The thickness of the gel correlates with conductivity, and thicker materials may reduce the efficiency of charge migration within the gel and affect conductivity. As shown in Fig. 4**c**, for thicknesses ranging from 450 to 650 μm and beyond, the sensitivity of the gel diminished with increasing thickness, which is aligned with the conductivity trend.

After determining the optimal type of ionic liquid and gel thickness, we investigated the effect of the mass fraction of the ionic liquid on the sensitivity and conductivity of the PVC gels (Fig. 4**e**). The sensitivity of the PVC gel strain sensors increased with an increase in the P/$[AMI]_mNTF_2$ ionic liquid mass fraction from 0 to 0.8 wt%. This trend was reflected in the conductivity profile (Fig. 4**f**), where the conductivity of the gel improved within the same ionic liquid content range. However, at an ionic liquid concentration of 1.6 wt%, the sensitivity of the ionic gel diminished compared to the 0.8 wt% P/$[AMI]_mNTF_2$, paralleling the trend in conductivity. On the other hand, it is also crucial to investigate the appropriate ratios of PVC and DBA, and the results show that the conductivity of PVC ionic gel decreases as the content of DBA increases (Fig. 4**h**), but the sensitivity of PVC12 is significantly lower than that of PVC14(Fig. 4**g**), which is attributed to the high electrical conductivity of PVC12, which leads to its reduced sensitivity to strain. Furthermore, we compared the sensing sensitivity of the same type of ionic gel (Fig. 4**i**) as well as the currently published PVC ionic gel (Table 1); the results showed that the PVC ionic gel in this study had better sensing sensitivity and higher conductivity.

SEM imaging confirmed that beyond an ionic liquid mass fraction of 0.8 wt%, the internal conductive pathways contracted, leading to reduced conductivity and diminished sensing performance. Equation S1 clarifies that the sensitivity of the PVC ionic gel is governed by the relative change in resistivity, a finding supported by experimental evidence. Therefore, charge transfer was promoted by increasing the ion concentration, modulating the PVC content to create more conductive channels for free ions as well as adjusting the thickness to improve the charge migration efficiency and sensing performance(Fig. S3). In conclusion, an ionic gel comprising 0.8 wt% P/$[AMI]_mNTF_2$ and a thickness of 450 μm emerged as a superior performer in terms of sensing capabilities. It achieved a GF of 27.8 (Fig. S8), and exhibited a conductivity of 4.84 ms/cm. The GF values were 8.3 and 19.5 in the 0–60 % and 60–120 % strain ranges, respectively, and increased notably to 27.8 in the 120–150 % strain range. This significant strain responsiveness was ascribed to alterations in the electrical resistance caused by changes in the geometry of the gel. As the gel is stretched, the consequent constriction of the ionic conductive pathways hinders charge migration, resulting in an elevated resistance.

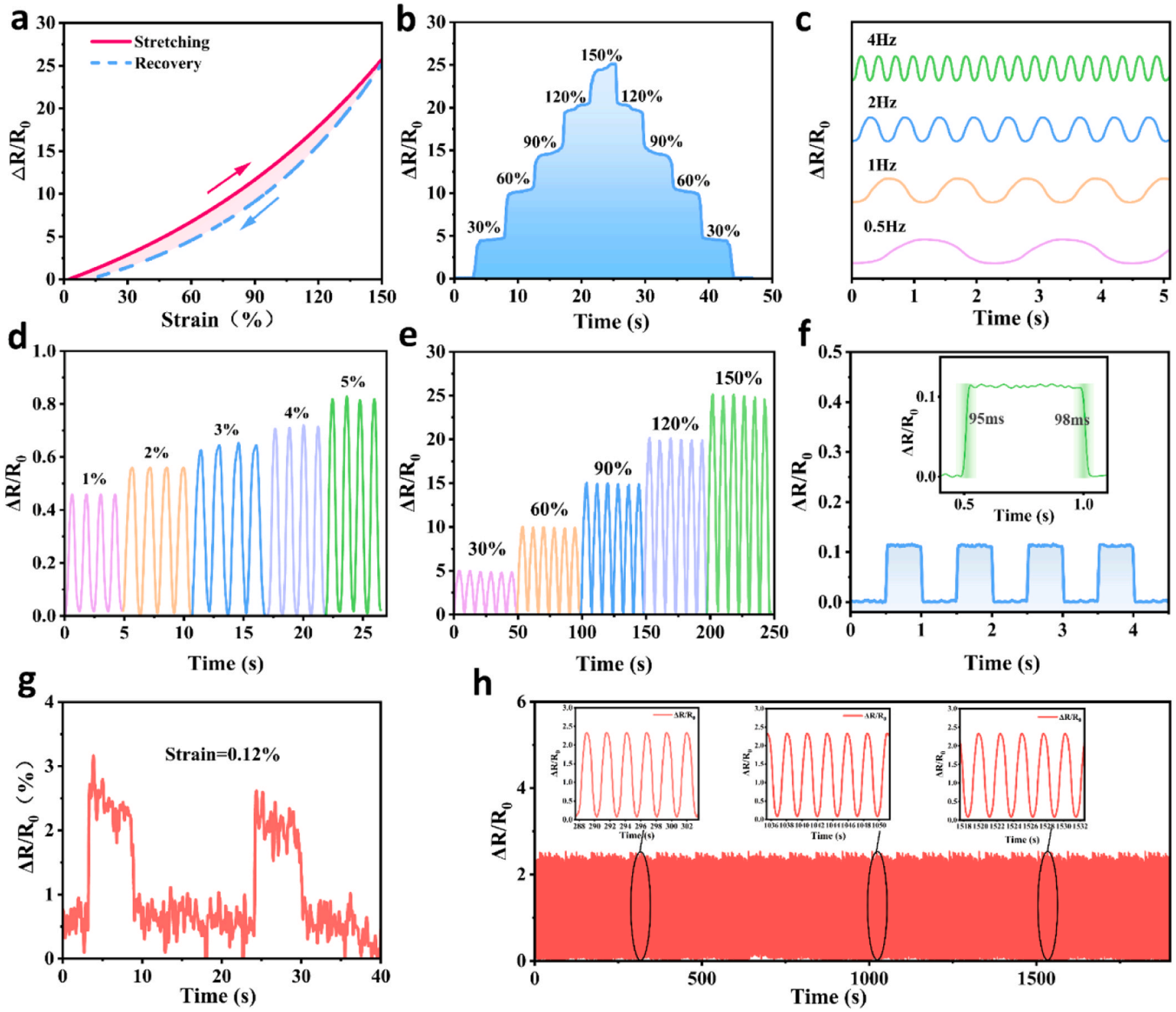

Fig. 5. Experiments on sensing performance of PVC ionic gels. (a) Sensitivity of the PVC ionic gels to different ion types. (b) Change in the resistance of the PVC ionic gel under step strain. (c) Resistance Change in resistance of the PVC ionic gel at 0.5 Hz~4 Hz strain rate. (d) Resistance variation of PVC ionic gel under 1 %-5 % strain. (e) Variation in the resistance of PVC ionic gel at 30 %-150 % strain. (f) Response time of PVC ionic gel. (g) Minimum strain resolution of PVC ionic gel. (h) Stability of PVC ionic gel at 1000 cycles.

3.3. PVC ionic gel sensing performance description

To evaluate the sensing performance of the PVC ionic gel, we designed a series of experiments to test the performance. Fig. 5**a** illustrates the characteristic output curves of the PVC ionic gel during the loading and unloading cycles, extending to a strain of 150 %. The non-overlapping signals indicate a hysteresis effect, which is characteristic of the mechanical properties of the material. Notably, the relative change in resistance during loading consistently exceeded that during unloading, suggesting a correlation with the inherent mechanical traits of the PVC ionic gel. Fig. 5**b** demonstrates the ability of the gel sensor to detect dynamic deformation. When subjected to successive gradient strains, the PVC ionic gel sensor responded quickly and accurately to larger strains, maintaining a stable relative change in resistance with a strain resolution of 30 %.

Further exploration of the dynamic electromechanical performance of the gel is presented in Fig. 5**c**, which depicts the dynamic stability of the gel under cyclically applied 30 % strain at frequencies ranging from 0.5 Hz to 4 Hz. The peak change in the relative resistance remained largely invariant with increasing frequency, demonstrating the robust dynamic characteristics of the gel and its excellent tensile rate responsiveness, which are crucial for strain sensor applications. Fig. 5**d-f** display the dynamic strain results, clearly indicating that the gel maintained a consistent resistance response across a broad strain spectrum (1 %-5 % in Fig. 5**d** and 30 %-150 % in Fig. 5**e**). Another important performance indicator is the response time of the sensor: fast gel response (~95 ms) and recovery (~98 ms) at 0.5 % strain, as shown in Fig. 5**f**, ensure fast adaptation to external strain without significant hysteresis. As depicted in Fig. 5**g**, at a cyclic strain of 10 %, the PVC ionic gel showed exceptional repeatability, stability, and durability over 1000 cycles. This research culminated in the development of PVC ionic-gel-based strain sensors characterized by high sensitivity, commendable repeatability across an extensive strain range, notable stretchability, and high resolution.

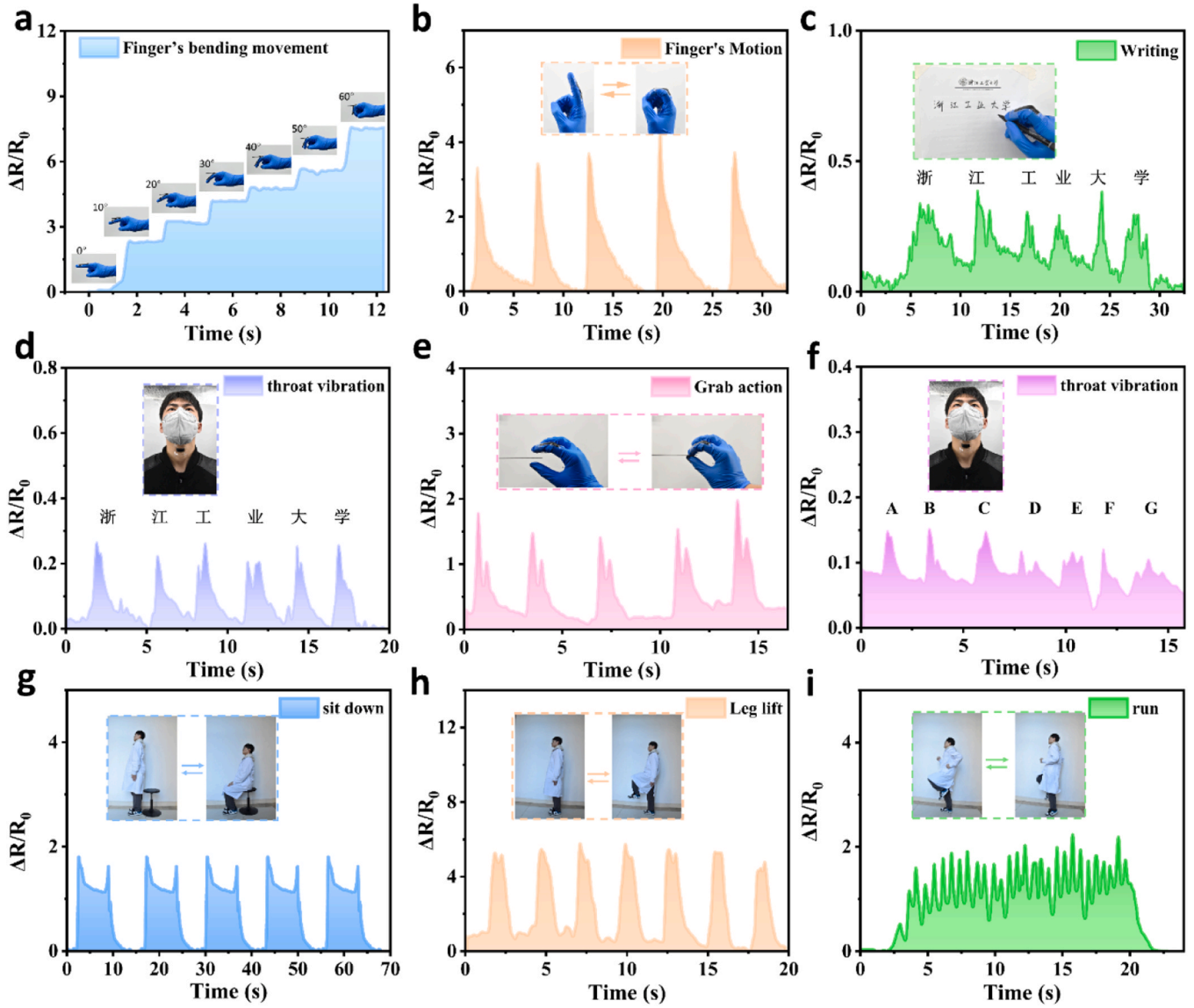

Fig. 6. Experimental applications of PVC ionic gels for wearable detection. (a) Detection of the finger bending angle. (b) Detection of bending and return motions of index finger. (c) Detection of finger movements during writing. (d) Detecting the motion of speaking Chinese at the throat. (e) Detection of English-speaking movements in the throat. (f) Detection of finger-grasping movements. (g) Detection of standing and sitting knee movements. (h) Detection of standing and bending knee movements. (I) Detection of running knee movements.

3.4. Wearable motion detection applications

In this study, we developed a signal acquisition and testing system, as illustrated in Fig. S4 to evaluate the efficacy of the PVC ionic gel as a sensor for wearable devices. The system capitalizes on the deformation of the PVC ionic gel caused by human motion to generate signals, demonstrating the exceptional sensing performance of the gel and its promising potential for human motion monitoring and wearable technologies. Fig. 6**a** shows the ability of the PVC ionic gel to detect subtle human body movements. The resistance of the gel changed gradually in response to varying finger bending angles, demonstrating its adept tracking capabilities. As presented in Fig. 6**b**, the PVC ionic gel could also monitor and detect the degree of finger flexion in real time, offering crucial support for remote operation of the robotic hand.

Moreover, PVC ionic gels can capture fine finger movement and vibrations. When affixed to a finger, the gel can consistently record finger motion. This is exemplified in Fig. 6**c**, where the gel successfully captured the vibration signals as the tester wrote Chinese characters for the “Zhejiang University of Technology” indicating the precise vibration recognition ability of the gel. Fig. 6**e** introduces a wearable device incorporating a PVC ionic gel as a sensor for daily human motion detection. Additionally, as shown in Fig. 6**d and f**, when saying the English letters "ABCDEFG" and the Chinese characters "Zhejiang University of Technology", the sensors generated a strain-induced signal caused by glottal movement, showing the potential for future applications in semantic recognition and rehabilitation training. The results of leg motion detection, detailed in Fig. 6**g-i**, further confirm the suitability of the gel for integration into wearable technology, given its high sensitivity and reliable performance over a wide range of motion. PVC ionic gel has been successfully used to monitor and record basic leg movements, including leg lifting, jumping, jogging, and stair climbing and descending. Each movement produced distinct and highly identifiable signal patterns. These findings underscore the capability of the gel to capture a comprehensive array of leg motions, each characterized by unique but easily identifiable signal profiles. The implications of these results are profound, suggesting that PVC ionic gels hold great promise for comprehensive motion monitoring of the human body. Their potential applications span a wide array of fields, including human-

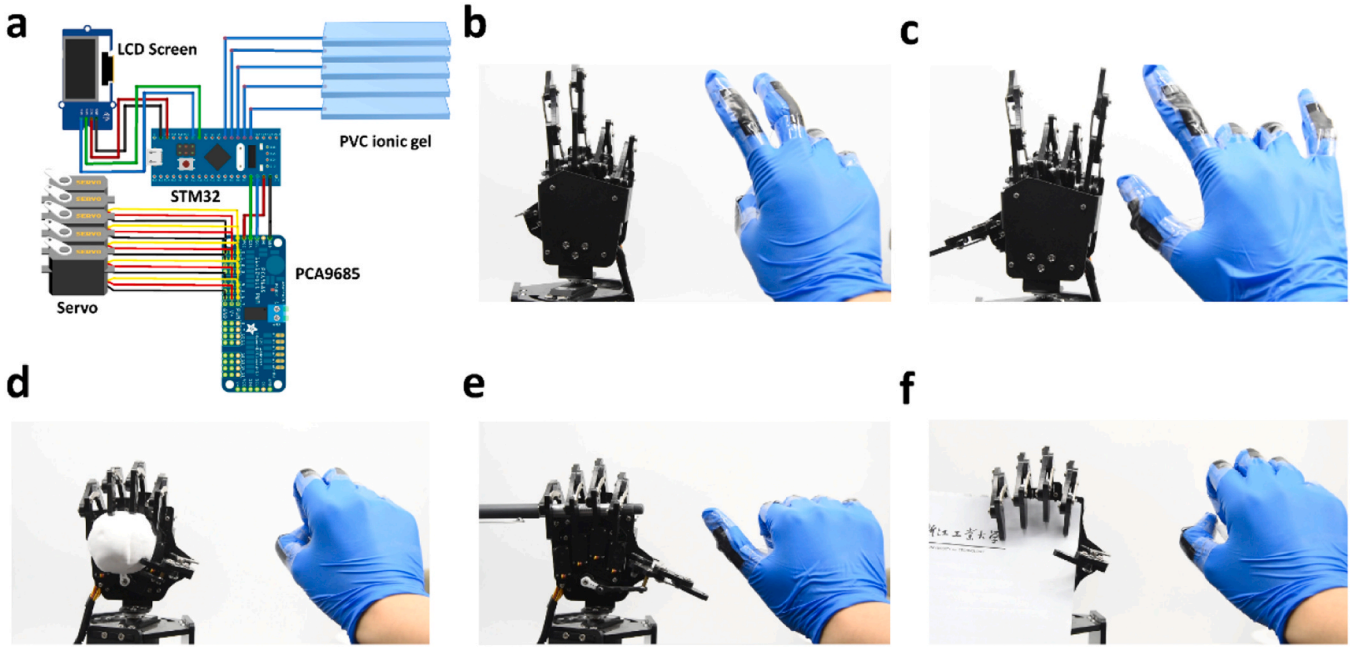

Fig. 7. PVC ionic gel for robotic hand applications. (a) System schematic for manipulating manipulator with PVC ionic gel. (b) Celebration gesture of the robotic hand. (c) Rock gesture of robotic hand. (d) Robotic hand gripping of spherical objects. (e) Robotic hand pen gripping. (f) Robotic hand-paper gripping.

computer interaction, wearable device integration, and sports risk assessment.

3.5. PVC ionic gel wearable sensors for robotic hand control

The results of this research underscore the suitability of PVC ionic gel wearable sensors for monitoring human motion energy, highlighting their potential in fields such as artificial intelligence and human-computer interaction. To further illustrate the practical applications of PVC ionic gel strain sensors in wearable interfaces, a smart glove was developed to monitor hand movements in real time.

This glove, equipped with five PVC ionic gel strain sensors measuring $50\times 10\times 0.5\ mm^2$ on each finger, successfully facilitated control of the manipulator, as demonstrated in Fig. 7**b**. The human-robot interface comprises two primary components: signal acquisition and robot execution. Detailed in Fig. 7**a**, the control system works on the principle that the gel detects finger deformation, and when the gel strain from finger bending reaches the corresponding resistance detection value, the acquisition circuit detects a voltage change. The microprocessor interprets the voltage change as an input signal and then uses pulse width modulation (PWM) to control the servo, thereby manipulating the motion of the robot. Interestingly, the robot is guided by a smart glove to perform several complex maneuvers. Besides, Fig. 7**d-e** depict the precise control capabilities of the robot, as it grasps objects during operation packing and remote control tasks. These actions confirm the ability of the manipulator to respond accurately to the external stimuli of the movements of the human body, and thus achieve an effective human-machine interaction. The results presented herein reveal the extensive application potential of PVC ionic gels in wearable flexible sensors. These sensors are capable of real-time monitoring of human body motion, paving the way for advancements in human-computer interaction technologies.

4. Conclusion

In conclusion, we have developed a high sensitivity and resolution flexible strain sensor based on a PVC ionic gel, which is formed by the physical blending of ionic liquids and PVC gel. In this study, we investigated the properties of ionic gel membranes.Subsequently, we explored the impact of various factors, the sensing performance was improved by increasing the ion concentration to promote charge transfer, adjusting the PVC content to create more conductive channels for free ions, and adjusting the thickness to increase the charge migration efficiency. The proposed sensor exhibited excellent sensing properties, including high sensitivity (GF of 27.8), high resolution (0.12 %) and commendable cycling durability over 1000 cycles at a strain of 10 %. Consequently, the sensor can successfully detect various human body movements and can be applied to the control of robotic hand. In the future, we will conduct a comprehensive study on the actuation and sensing properties of PVC gels. Overall, this work provides a new approach to address the low sensing performance of PVC gels and demonstrates the significant potential of PVC ionic gels in areas such as human-computer interaction, wearable devices, sports-related risk monitoring, and the integration of actuating and sensing.

CRediT authorship contribution statement

Yi Li: Conceptualization, Methodology, Funding acquisition, Project administration, Writing. **Ziqian Zhang**: Writing – original draft, Methodology, Investigation, Formal analysis, Data curation. **Lixiang Zhu**: Resources, Methodology. **Hangzhong Zhu**: Resources, Methodology. **Xia Zhang**: Validation, Supervision. **Mingfei Guo**: Supervision, Software. **Yanbiao Li**: Supervision, Funding acquisition, Project administration. **Minoru Hashimoto**: Validation, Supervision.

Declaration of Competing Interest

The authors declare that they have no known competing financial interests or personal relationships that could have appeared to influence the work reported in this paper.

Data availability

Data will be made available on request.

Acknowledgments

This work was supported by Zhejiang Provincial Natural Science Foundation of China (Grant No. LY22E050019), Ningbo Public Welfare Research Program Foundation of China (Grant No. 2023S066), the Science and Technology Research Program of Chongqing Municipal Education Commission (Grant No. KJZD-K201900702), the National Natural Science Foundation of China (Grant No. U21A20122), and the JSPS Grant-in-Aid for Scientific Research(C)(Grant No. JP22K04010).

Appendix A. Supporting information

Supplementary data associated with this article can be found in the online version at doi:10.1016/j.sna.2024.115826.

References

[1] M. Sui, Y. Ouyang, H. Jin, Z. Chai, C. Wei, J. Li, M. Xu, W. Li, L. Wang, S. Zhang, A soft-packaged and portable rehabilitation glove capable of closed-loop fine motor skills, Nat. Mach. Intell. 5 (2023) 1149–1160, https://doi.org/10.1038/s42256-023-00728-z.

[2] N. Bai, Y. Xue, S. Chen, L. Shi, J. Shi, Y. Zhang, X. Hou, Y. Cheng, K. Huang, W. Wang, J. Zhang, Y. Liu, C.F. Guo, A robotic sensory system with high spatiotemporal resolution for texture recognition, Nat. Commun. 14 (2023) 7121, https://doi.org/10.1038/s41467-023-42722-4.

[3] Y. Wang, H. Wu, L. Xu, H. Zhang, Y. Yang, Z.L. Wang, Hierarchically patterned self-powered sensors for multifunctional tactile sensing, Sci. Adv. 6 (2020) eabb9083, https://doi.org/10.1126/sciadv.abb9083.

[4] C. Tang, B. Du, S. Jiang, Q. Shao, X. Dong, X.-J. Liu, H. Zhao, A pipeline inspection robot for navigating tubular environments in the sub-centimeter scale, Sci. Robot. 7 (2022) eabm8597, https://doi.org/10.1126/scirobotics.abm8597.

[5] J. Liang, Y. Wu, J.K. Yim, H. Chen, Z. Miao, H. Liu, Y. Liu, Y. Liu, D. Wang, W. Qiu, Z. Shao, M. Zhang, X. Wang, J. Zhong, L. Lin, Electrostatic footpads enable agile insect-scale soft robots with trajectory control, Sci. Robot. 6 (2021) eabe7906, https://doi.org/10.1126/scirobotics.abe7906.

[6] M. Zhang, M. Wang, X. Zhang, C. Zhang, M. Li, S. Yu, Fabrication of a multilayered SGO/macroporous Nafion-based IPMC with enhanced actuation performance, Sens. Actuators B: Chem. 356 (2022) 131319, https://doi.org/10.1016/j.snb.2021.131319.

[7] H. Wang, L. Yang, Y. Yang, D. Zhang, A. Tian, Highly flexible, large-deformation ionic polymer metal composites for artificial muscles: fabrication, properties, applications, and prospects, Chem. Eng. J. 469 (2023) 143976, https://doi.org/10.1016/j.cej.2023.143976.

[8] H.S. Wang, J. Cho, H.W. Park, J.Y. Jho, J.H. Park, Ionic polymer–metal composite actuators driven by methylammonium formate for high-voltage and long-term operation, J. Ind. Eng. Chem. 96 (2021) 194–201, https://doi.org/10.1016/j.jiec.2021.01.021.

[9] S. Zhou, Z. Xu, Energy efficiency assessment of RCEP member states: a three-stage slack based measurement DEA with undesirable outputs, Energy 253 (2022) 124170, https://doi.org/10.1016/j.energy.2022.124170.

[10] X. Chu, M. Pang, R. Guan, W. Xu, W. Zhou, W. Ling, Electrochemical machining of variable wire diameter structure on smart micro SMA coil, J. Manuf. Process. 116 (2024) 315–328, https://doi.org/10.1016/j.jmapro.2024.02.065.

[11] H. Liu, R. Liu, K. Chen, Y. Liu, Y. Zhao, X. Cui, Y. Tian, Bioinspired gradient structured soft actuators: From fabrication to application, Chem. Eng. J. 461 (2023) 141966, https://doi.org/10.1016/j.cej.2023.141966.

[12] D. Guo, L. Wang, X. Wang, Y. Xiao, C. Wang, L. Chen, Y. Ding, PEDOT coating enhanced electromechanical performances and prolonged stable working time of IPMC actuator, Sens. Actuators B: Chem. 305 (2020) 127488, https://doi.org/10.1016/j.snb.2019.127488.

[13] K. Ke, M. McMaster, W. Christopherson, K.D. Singer, I. Manas-Zloczower, Highly sensitive capacitive pressure sensors based on elastomer composites with carbon filler hybrids, Compos. Part A: Appl. Sci. Manuf. 126 (2019) 105614, https://doi.org/10.1016/j.compositesa.2019.105614.

[14] M.A. Molod, P. Spyridis, F.-J. Barthold, Applications of shape memory alloys in structural engineering with a focus on concrete construction – a comprehensive review, Constr. Build. Mater. 337 (2022) 127565, https://doi.org/10.1016/j.conbuildmat.2022.127565.

[15] J. Xue, Y. Ge, Z. Liu, Z. Liu, J. Jiang, G. Li, Photoprogrammable moisture-responsive actuation of a shape memory polymer film, ACS Appl. Mater. Interfaces 14 (2022) 10836–10843, https://doi.org/10.1021/acsami.1c24018.

[16] Y. Sato, Y. Guo, Shape-memory-alloys enabled actuatable fiber sensors via the preform-to-fiber fabrication, ACS Appl. Eng. Mater. 1 (2023) 822–831, https://doi.org/10.1021/acsaenm.2c00226.

[17] A. Iannarelli, M. Ghaffarian Niasar, R. Ross, Electrode interface polarization formation in dielectric elastomer actuators, Sens. Actuators A: Phys. 312 (2020) 111992, https://doi.org/10.1016/j.sna.2020.111992.

[18] Y. Li, M. Guo, Y. Li, Recent advances in plasticized PVC gels for soft actuators and devices: a review, J. Mater. Chem. C 7 (2019) 12991–13009, https://doi.org/10.1039/C9TC04366G.

[19] C. Dong, Z. Zhu, Z. Li, X. Shi, S. Cheng, P. Fan, Design of fishtail structure based on oscillating mechanisms using PVC gel actuators, Sens. Actuators A: Phys. 341 (2022) 113588, https://doi.org/10.1016/j.sna.2022.113588.

[20] Y. Li, M. Hashimoto, PVC gel soft actuator-based wearable assist wear for hip joint support during walking, Smart Mater. Struct. 26 (2017) 125003, https://doi.org/10.1088/1361-665X/aa9315.

[21] C. Liu, J.J.C. Busfield, K. Zhang, An electric self-sensing and variable-stiffness artificial muscle, Adv. Intell. Syst. 5 (2023) 2300131, https://doi.org/10.1002/aisy.202300131.

[22] H. Ling, S. Liu, Z. Zheng, F. Yan, Organic flexible electronics, Small Methods 2 (2018) 1800070, https://doi.org/10.1002/smtd.201800070.

[23] J. Neubauer, K.J. Kim, Multiphysics modeling framework for soft PVC gel sensors with experimental comparisons, Polymers 15 (2023) 864, https://doi.org/10.3390/polym15040864.

[24] G. Hwang, J. Nam, M. Kim, D.S. Diaz Cortes, K. Kyung, Protective and collision-sensitive gel-skin: visco-elastomeric polyvinyl chloride gel rapidly detects robot collision by breaking electrical charge accumulation stability, Adv. Intell. Syst. (2024) 2300583, https://doi.org/10.1002/aisy.202300583.

[25] Q. He, Q. Zhong, Z. Sun, H. Zhang, Z. Zhao, Z. Shi, X. Liu, Z. Zhao, J. Lu, Y. Ye, Y. Wang, Y. Li, T. Xiang, J. Zhao, Y. Xie, Highly stretchable, repeatable, and easy-to-prepare ionogel based on polyvinyl chloride for wearable strain sensors, Nano Energy 113 (2023) 108535, https://doi.org/10.1016/j.nanoen.2023.108535.

[26] Y.J. Son, J.W. Bae, H.J. Lee, S. Bae, S. Baik, K.-Y. Chun, C.-S. Han, Humidity-resistive, elastic, transparent ion gel and its use in a wearable, strain-sensing device, J. Mater. Chem. A 8 (2020) 6013–6021, https://doi.org/10.1039/D0TA00090F.

[27] Q. Xu, Z. Wu, W. Zhao, M. He, N. Guo, L. Weng, Z. Lin, M.F.A. Taleb, M.M. Ibrahim, M.V. Singh, J. Ren, Z.M. El-Bahy, Strategies in the preparation of conductive polyvinyl alcohol hydrogels for applications in flexible strain sensors, flexible supercapacitors, and triboelectric nanogenerator sensors: an overview, Adv. Compos Hybrid. Mater. 6 (2023) 203, https://doi.org/10.1007/s42114-023-00783-5.

[28] Y. Li, X. Feng, L. Zhu, Z. Zhang, M. Guo, Y. Li, M. Hashimoto, High performance fiber-constrained plasticized PVC gel actuators for soft robotics, Sens. Actuators B: Chem. 393 (2023) 134177, https://doi.org/10.1016/j.snb.2023.134177.

[29] Z. Wang, Y. Wang, Z. Wang, Q. He, C. Li, S. Cai, 3D printing of electrically responsive PVC gel actuators, ACS Appl. Mater. Interfaces 13 (2021) 24164–24172, https://doi.org/10.1021/acsami.1c05082.

[30] B. Zheng, X. Man, D. Andelman, M. Doi, Enhanced electro-actuation in dielectric elastomers: the nonlinear effect of free ions, ACS Macro Lett. 10 (2021) 498–502, https://doi.org/10.1021/acsmacrolett.1c00045.

[31] J. Neubauer, Z.J. Olsen, Z. Frank, T. Hwang, K.J. Kim, A study of mechanoelectrical transduction behavior in polyvinyl chloride (PVC) gel as smart sensors, Smart Mater. Struct. 31 (2022) 015010, https://doi.org/10.1088/1361-665X/ac358f.

[32] Z. Liu, B. Li, Y.D. Liu, Y. Liang, Integrated bending actuation and the self-sensing capability of poly(vinyl chloride) gels with ionic liquids, Adv. Funct. Mater. 32 (2022) 2204259, https://doi.org/10.1002/adfm.202204259.

[33] Y. Wang, Y. Xia, P. Xiang, Y. Dai, Y. Gao, H. Xu, J. Yu, G. Gao, K. Chen, Protein-assisted freeze-tolerant hydrogel with switchable performance toward customizable flexible sensor, Chem. Eng. J. 428 (2022) 131171, https://doi.org/10.1016/j.cej.2021.131171.

[34] J. Huang, X. Zhang, R. Liu, Y. Ding, D. Guo, Polyvinyl chloride-based dielectric elastomer with high permittivity and low viscoelasticity for actuation and sensing, Nat. Commun. 14 (2023) 1483, https://doi.org/10.1038/s41467-023-37178-5.

Yi Li received the M.S. and Ph.D. degrees from Shinshu University, Japan, in 2010 and 2016, respectively. He is currently an associate professor at the College of Mechanical Engineering, Zhejiang University of Technology, Hangzhou, China. His current research interests include artificial muscles and applications in motion-assist systems.

Ziqian Zhang received his bachelor's degree in 2021 from Xiangtan University, China. He is currently a postgraduate student in Zhejiang University of Technology. His research interests include soft electrodes and actuators.

Lixiang Zhu received his bachelor's degree in 2021 from Zhongyuan University of Technology, China. He is currently a postgraduate student at the Zhejiang University of Technology. His research interests include soft actuators and robotics research.

Hangzhong Zhu received his bachelor's degree in 2023 from Zhejiang A&F University, China. He is currently a postgraduate student in Zhejiang University of Technology. His research interests include soft sensors and actuators.

Xia Zhang received the Ph.D. degrees from Shinshu University, Japan, in 2012. She is currently a professor at the School of Mechatronics and Vehicle Engineering, Chongqing Jiaotong University, China. Her research interests include robotics and artificial muscles.

Mingfei Guo received his master. degree from Shandong University, China, in 2002. He is currently a lecturer at the College of Mechanical Engineering, Zhejiang University of Technology, China. His research interests include soft actuators and robotics.

Yanbiao Li received his Ph.D. degree from Yanshan University, China, in 2008. He is currently a professor at the College of Mechanical Engineering, Zhejiang University of

Technology, China. His research interests include parallel mechanisms, artificial muscles and robotics.

Minoru Hashimoto received M.S. and Ph.D. degrees from the University of Tokyo in 1980 and 1983, respectively. He is currently a specially appointed professor at the Faculty of Textile Science and Technology, Shinshu University. His research interests include artificial muscles and wearable robotics. He is a member of IEEE.